Available online at www.sciencedirect.com
SCIENCE DIRECT®
Solar Energy Materials & Solar Cells
ELSEVIER
Solar Energy Materials & Solar Cells 83 (2004) 263–271
www.elsevier.com/locate/solmat

Improving power efficiencies in polymer—polymer blend photovoltaics

A.J. Breeze[a], Z. Schlesinger[b], S.A. Carter[b,*], H. Tillmann[c], H.-H. Hörhold[c]

[a] *National Renewable Energy Laboratory, Golden, CO 80401, USA*
[b] *Physics Department, University of California, Santa Cruz, CA 95064, USA*
[c] *Friedrich - Schiller - Universität, Jena, Germany*

Abstract

The use of blends of electron and hole transporting polymers has been shown to increase exciton dissociation and efficiency in polymer-based photovoltaics. We compare plain M3EH-PPV devices to M3EH-PPV:CN-ether-PPV blend devices, demonstrating the improved performance of blends. We vary the polymer layer thickness and device electrodes for M3EH-PPV:CN-ether-PPV polymer blend devices to investigate the factors limited device efficiency. We find that although the blends allow exciton dissociation to take place throughout the polymer layer, these devices are still limited by transport properties rather than by light absorption. Our best blend device, made with indium-tin oxide and Ca electrodes, gives a power conversion efficiency $\eta_p = 1.0\%$.

Keywords: Polymer solar cells; Polymer blends; Charge transport; Carrier mobility; Exciton dissociation; M3EH-PPV; CN-ether-PPV; Titanium dioxide solgel

1. Introduction

Since the discovery of polyacetylene in 1977, semiconducting polymers have been investigated for various applications including light emitted diodes and photovoltaics due to their promise of low cost, less toxic manufacturing methods, tunable optical properties, and the possibility of light weight, flexible large-area panels. Extended work on electronic injection and transport, optoelectric properties and

*Corresponding author. Tel.: +1-831-459-3043.
E-mail address: sacarter@cats.ucsc.edu (S.A. Carter).

0927-0248/$ - see front matter © 2004 Published by Elsevier B.V.
doi:10.1016/j.solmat.2004.02.029

material purification has allowed polymer LED power conversion efficiencies to approach those of their inorganic counterparts. However, polymer solar cell efficiencies are still far below those of amorphous silicon or dye sensitized electrochemical cells [1].

Short exciton diffusion lengths and low carrier mobilities have been shown to be two of the greater limiting factors impeding higher power conversion efficiencies (η_p) in polymer-based photovoltaic systems. Photons absorbed in the polymer layer create bound electron–hole pairs which must be dissociated before recombination occurs in order to collect charge from the device. Due to the relatively low internal field strengths in these devices, this process occurs at dissociation sites; generally, these are at the interface between materials of high electron affinity and low ionization potential [2,3]. Therefore, in polymer devices consisting of a single polymer layer sandwiched between two electrodes of differing workfunctions, charge collection is restricted to the polymer area within an exciton diffusion length of either of the electrodes. Recombination and hence loss of efficiency dominates the light absorption in the middle of the polymer layer.

Various approaches have been explored in an effort to circumvent this restriction. Nanoparticle/nanocrystal—polymer blends [4–7] and polymer–polymer blends of electron and hole transporting polymers [8–12] show promise for increasing exciton dissociation. By blending polymers of appropriate energy levels together in a common solvent and spin casting from a single solution, phase separation on the nanometer scale can be achieved, creating dissociation interfaces throughout the entire polymer layer [8,10]. This paper addresses the question of whether or not the increase in dissociation is sufficient to put these devices in the realm of being light absorption limited or if the efficiencies are still limited by charge transport in one way or another. To do this, we examine the current density–voltage (J–V) characteristics as a function of polymer thickness and electrode choice. We also compare the performance of single polymer solar cells with the polymer–polymer blend devices.

2. Experimental

Devices are composed of thin films of sintered titanium dioxide (TiO_2) solgel and polymer between indium tin oxide (ITO) and gold electrodes in a sandwich structure. The TiO_2 solgel precursor, prepared as described elsewhere [13], is spun at 1000 rpm over commercial ITO patterned glass slides to a thickness of about 50 nm. The mostly transparent films are baked at 450°C under normal atmosphere for 1 h to remove the remaining solvent and convert the film structure to crystal anatase. Atomic force microscopy (AFM) images show the films to be very smooth, with surface roughness on the order of 2 nm [14]. The polymers M3EH-PPV [15] and CN-ether-PPV [16] (Fig. 1) are mixed in a 1:1 weight ratio for a 10 g/l solution in chlorobenzene. The polymer solution is spun at speeds of 3000, 2000, and 1000 rpm to create film thicknesses of 45, 60 and 85 nm, respectively. The resulting films are baked under low vacuum at 125°C for one hour to remove the solvent and to anneal the films. The thicknesses of both the polymer and TiO_2 films are measured by AFM.

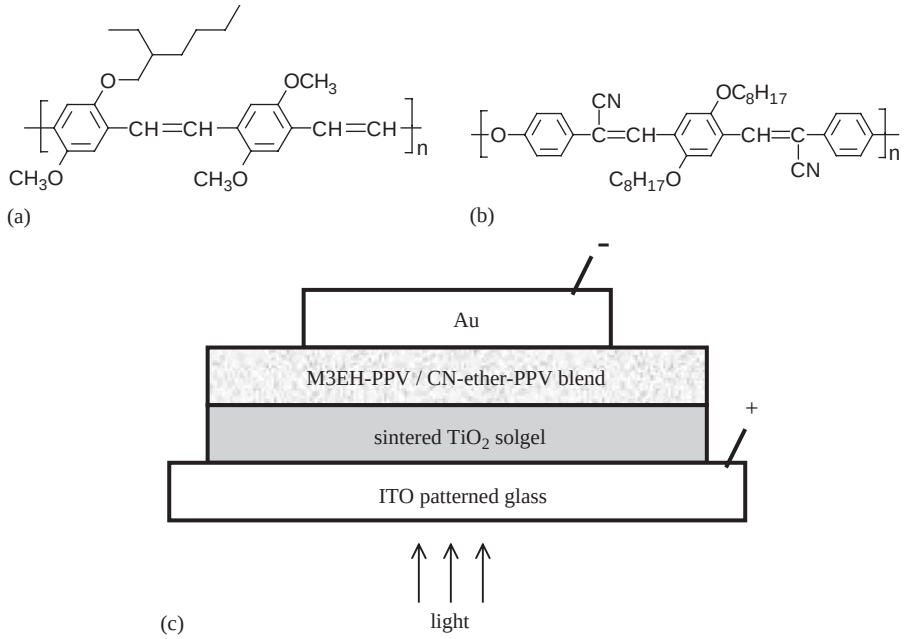

Fig. 1. The chemical diagrams for the polymers (a) M3EH-PPV and (b) CN-ether-PPV. (c) Structure for an ITO/TiO_2/polymer blend/Au layered device.

At this point the samples are brought into a nitrogen atmosphere glove box where the top gold electrode (50–70 nm) is evaporated. Devices made using Al or Ca as the top electrode are constructed in the same manner, with the conducting polymer PEDOT replacing the TiO_2 layer [17]. The device area is 3 mm^2 with six devices per substrate to check reproducibility.

Current density–voltage curves are taken both in the dark and under white illumination using a Keithley 2400 source meter by sourcing voltage such that ITO is positive and Au is negative in forward bias. Illumination of approximately 80 mW/cm^2 is provided by a xenon light bulb, the intensity of which is measured using a calibrated silicon solar cell. Photocurrent action spectra are taken at zero bias and low light intensities using a halogen light source, monochromator, chopper and a lock-in amplifier, with reference spectra provided by the silicon solar cell. To prevent oxygen from diffusing into the polymer and creating additional charge traps, all electronic measurements are taken in a dry nitrogen atmosphere. Absorption spectra of the polymer films are taken with an N & K optical spectrometer.

3. Results and discussion

M3EH-PPV is by itself an improved photovoltaic polymer, yielding short-circuit current densities J_{sc} of 1.2 mA/cm^2 (Fig. 2), noticeably higher than the 150 μA/cm^2

measured for MEH-PPV solar cells of similar device structure [14]. To understand better this increase in performance, we investigated the hole mobility in M3EH-PPV. Charge transport in semi-conducting polymers is observed to be space-charge limited:

$$J = 98\ \epsilon\mu E^2/L, \tag{1}$$

where μ is the field-dependent mobility, E is the electric field, L is the thickness of the semi-conducting polymer layer, and the permittivity ε is assumed to be 3.1×10^{-11} C^2/Nm^2, similar to that of MEH-PPV. It should be noted that this is the trap-free form of the space-charge limited current. Studies have shown that hole mobilities in this class of polymer yield a field-independent activated mobility at low field strengths, with a transition to a field-dependent mobility at higher field strengths [18]. The field-dependent mobility can be fit to a stretched exponential expression:

$$\mu_0 = \mu_0 \exp(0.89\ \gamma\ \mathrm{sqrt}(E)). \tag{2}$$

A more detailed analysis and explanation of this type of fit can be found in Ref. [19] and references therein. Hole mobility in M3EH-PPV is measured in the range of 3.9–6.35 V using an ITO/PEDOT/M3EH-PPV/Al device by fitting J–V curves to Eqs. (1) and (2) (Fig. 3). PEDOT acts as a conducting electrode in this device and does not

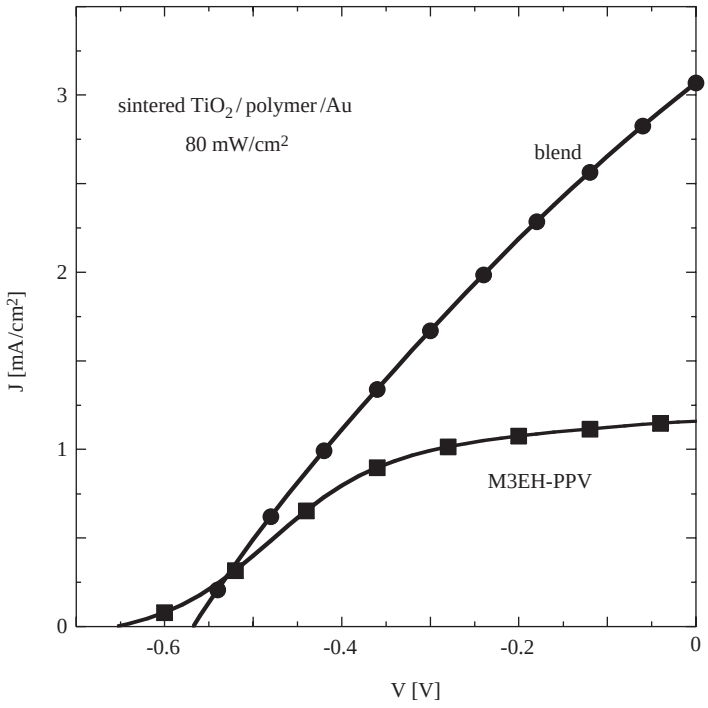

Fig. 2. J–V curves taken at 80 mW/cm^2 for devices ITO/TiO_2/M3EH-PPV:CN-ether-PPV/Au (circles) and ITO/TiO_2/M3EH-PPV/Au (squares), both with 40 nm polymer layers.

directly affect the space-charge limited current in the M3EH-PPV layer other than in the determination of the built-in-field across the device. Fits to the data yield an average hole mobility of 5.1×10^{-7} cm^2/Vs, just under twice that of similar annealed MEH-PPV [14]. This increase in mobility does not completely account for the improvement in short-circuit current density over MEH-PPV devices; it is possible that the M3EH-PPV devices also have slightly increased exciton dissociation efficiencies and/or exciton diffusion lengths.

Current density–voltage curves comparing a control device of M3EH-PPV with an M3EH-PPV: CN-ether-PPV blend, each with 40 nm polymer layers and using the TiO_2/Au structure, are shown in Fig. 2. (The current densities measured for CN-ether-PPV control devices degraded too quickly to make reasonable measurements. As shown in Fig. 2, an M3EH-PPV:CN-ether-PPV blend device of corresponding thickness has $J_{sc} = 3.1$ mA/cm^2. Assuming an exciton diffusion length of 15–20 nm [20], this factor of 2.5 increase in J_{sc} is consistent with exciton dissociation occurring through a majority of the polymer thickness for the blend devices. Our best ITO/TiO_2/M3EH-PPV:CN-ether-PPV blend/Au devices, made with a polymer thickness of 45 nm, have achieved $J_{sc} = 3.3$ mA/cm^2 and open-circuit voltage $V_{oc} = -0.65$ V, leading to an overall conversion efficiency of 0.75%.

There is a drawback, however, to the use of polymer–polymer blends. While the exciton dissociation is increased, leading to substantial increases in current, there is

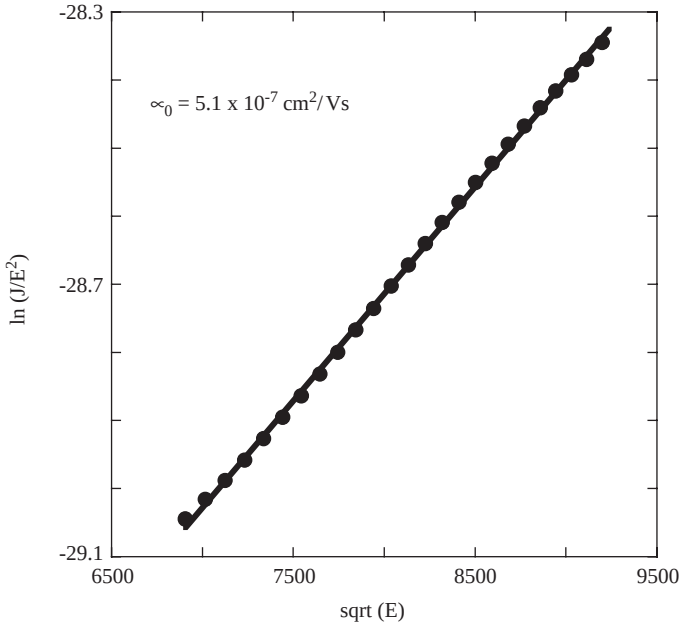

Fig. 3. A representative data set for space-charge limited current density in the field-dependent mobility regime for an ITO/PEDOT/M3EH-PPV/Al device: a linear fit of $\ln(J/E^2)$ vs. sqrt(E) gives the field-independent mobility term μ_0. The electric field $E = V_{ap} - V_{bi}$ takes into account both the applied voltage V_{ap} and the built-in voltage V_{bi} (0.8 V) created by the difference in electrode workfunctions.

no corresponding increase in the carrier mobility. Since the fill-factor can be thought of as roughly proportional to the carrier mobility and inversely proportional to the short-circuit current density, the increase in photocurrent with no corresponding mobility increase leads to much lower fill factors, going from on the order of 40% for plain M3EH devices to 28% for blend devices. There is also the possible issue of each polymer creating continuous percolation pathways for each carrier type between the electrodes, contributing to somewhat lower rectification ratios and hence lower fill factors [21]. Even so, polymer–polymer blends have higher efficiency compared to single polymer devices; the plain 40 nm M3EH-PPV device has an $\eta_p = 0.40\%$, while the comparable polymer blend device has $\eta_p = 0.62\%$. Fig. 4 shows the external quantum efficiency as a function of wavelength for devices made using the polymer blend, plain M3EH-PPV and plain MEH-PPV. The blend's peak quantum efficiency, 23.5%, is close to that of laminated layered polymer blends using ITO and Al electrodes [8].

To further examine whether the efficiency of the polymer blend devices is limited by dissociation, we consider different electrode configurations. For plain polymer devices, it has been shown that the choice of electrodes and hence the direction of the internal field makes an order of magnitude difference to the device performance [13, 14]. This is caused by the disparity between the hole and electron mobilities and by the fact that exciton dissociation is limited to the area within a diffusion length of the contacts. We have examined three different electrode configurations: ITO/TiO_2/polymer blend/Au, ITO/PEDOT/polymer blend/Al and ITO/PEDOT/polymer

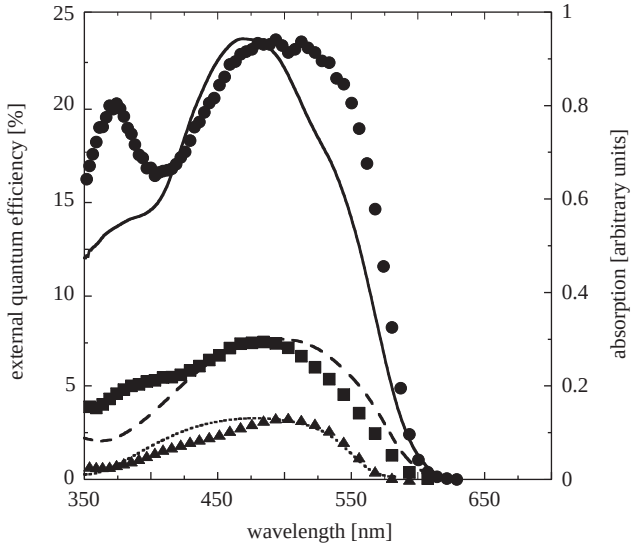

Fig. 4. The external quantum efficiency as a function of wavelength for M3EH-PPV (squares), MEH-PPV (triangles) and 1:1 M3EH-PPV:CN-ether-PPV (circles) devices using the TiO_2/Au structure. The absorption spectra for M3EH-PPV (dashed line), MEH-PPV (dotted line) and 1:1 M3EH-PPV:CN-ether-PPV blend (line) are also shown.

blend/Ca, all with 60 nm polymer thicknesses. The lower workfunction of Ca (2.87 eV [22]) gives that device a larger internal bias in the same direction as the Al device. The TiO_2/polymer blend/Au device has an internal field in the opposite direction. Unlike plain polymer devices, the blends show no great variation in performance for the different electrode configurations, supporting the theory that the blends allow for exciton dissociation throughout the polymer thickness (Fig. 5). The Ca device, with its larger internal bias, gives $J_{sc} = 3.2\,mA/cm^2$, $V_{oc} = -1.0\,V$ and a fill factor = 25%, for a conversion efficiency of 1.0%.

We vary the thickness of the polymer blend layer in order to determine whether it is light absorption or charge transport that limits the conversion efficiency of these devices. ITO/TiO_2/polymer blend/Au devices are made with polymer thicknesses of 45, 60 and 85 nm. Short-circuit current densities range from $1.7\,mA/cm^2$ for the 85 nm device to $3.3\,mA/cm^2$ for the 45 nm device, with fill-factors of 27–28% and V_{oc} ranging from -0.65 to $-0.78\,V$ (Fig. 6). Similar to plain polymer devices [14], short-circuit current density for the blend devices increases with decreasing polymer thickness. We interpret this to mean that the performance of the polymer blend samples is still limited by charge transport, most likely resistive losses and low carrier mobilities across the polymer layer, rather than by light absorption. Maximum

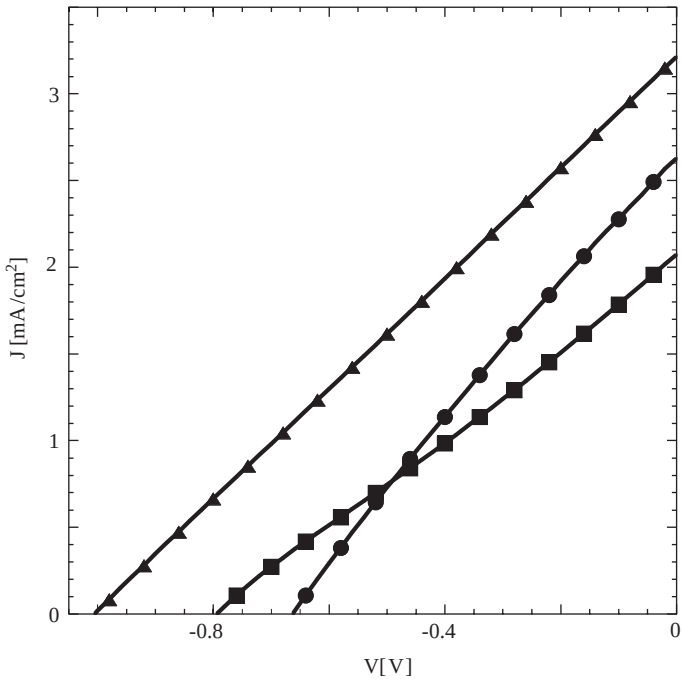

Fig. 5. $J-V$ curves taken at $80\,mW/cm^2$ for devices ITO/TiO_2/M3EH-PPV:CN-ether-PPV/Au (circles), ITO/PEDOT/M3EH-PPV:CN-ether-PPV/Al (squares) and ITO/PEDOT/M3EH-PPV:CN-ether-PPV/Ca (triangles). The polarity of the applied voltage has been reversed for the Al and Ca devices for comparison with the Au device.

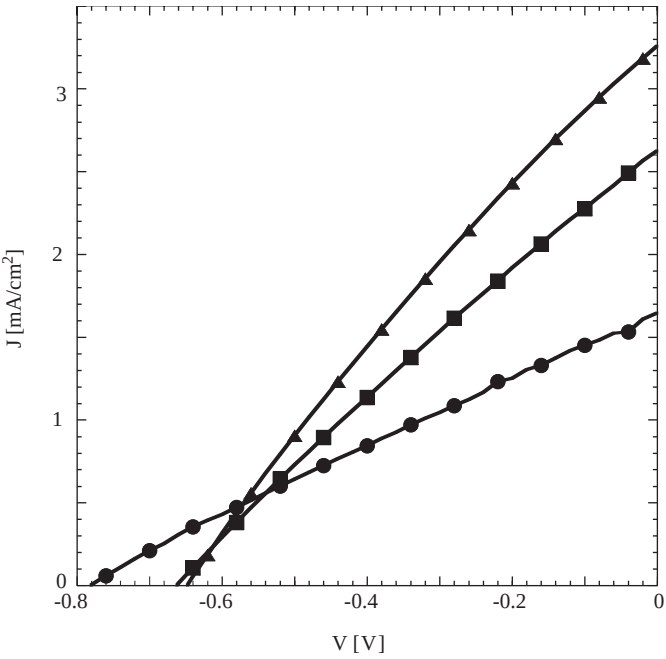

Fig. 6. *J–V* curves taken at 80 mW/cm^2 for ITO/TiO_2/M3EH-PPV:CN-ether-PPV/Au devices with polymer thicknesses of 85 nm (circles), 60 nm (squares) and 45 nm (triangles).

absorption coefficients in these polymers are on the order of 0.017 nm^{-1}, and so for a 60 nm layer only about 60% of the incident light is absorbed in the polymer blend layer at the maximum absorbing wavelength. Therefore, we would expect the photocurrent to increase with increasing polymer thickness if the devices were absorption limited.

4. Conclusions

In conclusion, we have confirmed previous results showing that hole and electron transporting polymers blended in a common solvent and spun to create a film with phase separation on the nanometer scale leads to increased exciton dissociation and therefore to higher photocurrents and power conversion efficiencies. New polymers, most notably M3EH-PPV, show good improvement over the more traditional polymers such as MEH-PPV which were developed for LED rather than photovoltaic properties. Single polymer devices using M3EH-PPV have yielded overall conversion efficiencies of 0.40% using a TiO_2/polymer/Au configuration, while blends of M3EH-PPV and CN-ether-PPV give 0.75% efficiencies for the same electrodes and 1.0% for PEDOT and Ca electrodes. By varying the electrodes, we have shown that polymer blends eliminate a great deal of the limitation caused by low exciton diffusion lengths. However, variation of the polymer blend layer

thickness demonstrates that these devices are still limited more by charge transport, likely low mobilities and resistive losses across the polymer layer, than they are by light absorption in the polymer. It will be necessary to improve all of these factors in order to make viable plastic solar cells.

References

[1] B. O'Regan, M. Gratzel, Nature 353 (1991) 737–740.
[2] C.W. Tang, Appl. Phys. Lett. 48 (1986) 183–185.
[3] R.H. Friend, G.J. Denton, J.J.M. Halls, N.T. Harrison, A.B. Holmes, A. Kohler, A. Lux, S.C. Moratti, K. Pichlet, N. Tessler, K. Towns, Synth. Met. 84 (1997) 463–470.
[4] N.C. Greenham, X. Peng, A.P. Alvisatos, Phys. Rev. B 54 (1996) 17628–17637.
[5] W.U. Huynh, X. Peng, P.A. Alivisatos, Adv. Mater. 11 (1999) 923–927.
[6] G. Yu, J. Gao, J.C. Hummelen, F. Wudl, A.J. Heeger, Science 270 (1995) 1789–1791.
[7] F. Padinger, R.S. Rittberger, N.S. Sariciftci, Adv. Funct. Mater. 13 (2003) 85–88.
[8] M. Granstrom, K. Petritsch, A.C. Arias, A. Lux, M.R. Andersson, R.H. Friend, Nature 395 (1998) 257–260.
[9] J. Gao, G. Yu, A.J. Heeger, Adv. Mater. 10 (1998) 692–695.
[10] J.J.M. Halls, C.A. Walsh, N.C. Greenham, E.A. Marsegila, R.H. Friend, S.C. Moratti, A.B. Holmes, Nature 376 (1995) 498–500.
[11] W. Feng, A. Fujii, S. Lee, H. Wu, K. Yoshino, J. Appl. Phys. 88 (2000) 7120–7123.
[12] G. Yu, A.J. Heeger, J. Appl. Phys. 78 (1995) 4510–4515.
[13] A.C. Arango, L.R. Johnson, V.N. Bliznyuk, Z. Schlesinger, S.A. Carter, H.-H. Horhold, Adv. Mater. 12 (2000) 1689–1692.
[14] A.J. Breeze, Z. Schlesinger, P.J. Brock, S.A. Carter, Phys. Rev. B 64 (2001) 125205.
[15] S. Pfeiffer, H.-H. Horhold, Macromol. Chem. Phys. 200 (1999) 1870–1878.
[16] H. Tillmann, H.-H. Horhold, Synth. Met. 101 (1999) 138–139.
[17] S.A. Carter, M. Angelopoulos, S. Karg, P.J. Brock, J.C. Scott, Appl. Phys. Lett. 70 (1997) 2067–2069.
[18] P.W.M. Blom, M.C.J.M. Vissenberg, Mater. Sci. Eng. R. 27 (2000) 53–94.
[19] L. Bozano, S.A. Carter, J.C. Scott, G.G. Malliaras, P.J. Brock, Appl. Phys. Lett. 74 (1999) 1132–1134.
[20] T.J. Savenije, J.M. Warman, A. Goossens, Chem. Phys. Lett. 287 (1998) 148–153.
[21] L. Chen, D. Godovsky, O. Inganas, J.C. Hummelen, R.A.J. Janssens, M. Svensson, M.R. Andersson, Adv. Mater. 12 (2000) 1367–1370.
[22] Weast, R.C. (Ed.), Handbook of Chemistry and Physics, CRC Press, Inc., Boca Raton, 1989.